

[V₁₆Sb₄O₄₂(H₂O){VO(C₆H₁₄N₂)₂]₄]: A Terminal Expansion to a Polyoxovanadate Archetype

Adam Wutkowski,[†] Christian Näther,[†] Paul Kögerler,[‡] and Wolfgang Bensch^{*†}

Institut für Anorganische Chemie, Christian-Albrechts-Universität zu Kiel, Olshausenstrasse 40, D-24098 Kiel, Germany, and Institut für Anorganische Chemie, RWTH Aachen, D-52074 Aachen, Germany

Received January 10, 2008

The charge-neutral antimonatopolyoxovanadium(IV) cluster [V₁₆Sb₄O₄₂(H₂O){VO(C₆H₁₄N₂)₂]₄ · 10H₂O · C₆H₁₄N₂ was obtained under solvothermal conditions. The central cluster fragment, [V₁₆Sb₄O₄₂], is a derivative of the [V₁₈O₄₂] archetype and is formed by replacing two VO₅ polyhedra by two Sb₂O₅ units. The {V₂₀Sb₄} structure expands the {V₁₆Sb₄} motif by the addition of four square-pyramidal, terminal VO(1,2-diaminocyclohexane)₂ groups. At low temperatures, the magnetic ground state is characterized by four independent S = 1/2 sites.

Reduced polyoxovanadates form a class of molecular metal oxide compounds that feature unique aspects, e.g., catalytic deNO_x properties,¹ inorganic supramolecular host–guest chemistry with a flexible structural complementarity,² a vast redox chemistry characterized by different cluster types existing in various reduction states,³ and, because of the presence of d¹ vanadyl (VO²⁺; spin 1/2) groups, magnetic properties that render several such cluster compounds as important model systems for the study of, e.g., spin frustration,⁴ Dzyaloshinsky–Moria interactions and other splitting effects,⁵ or spin–phonon bottlenecks and butterfly hysteresis.⁶ In this context, several arsenate polyoxovanadates have been studied extensively, most prominently the D₃-symmetric

polyoxovanadate cluster anion [V^{IV}₁₅As^{III}₆O₄₂(H₂O)]^{6–},⁷ representing an equilateral spin 1/2 triangle. Although fully reduced, i.e., comprising 15 S = 1/2 sites, the {V₁₅As₆} system falls into two strongly antiferromagnetically coupled V₆ hexagons⁸ that sandwich a V₃ triangle featuring weak intratriangle coupling via O₂As(μ-O)AsO₂ superexchange pathways. Antisymmetric exchange coupling causes splitting of the doublet ground state and a pronounced magnetic anisotropy, dominating the low-temperature magnetism of {V₁₅As₆}.⁹

To expand the array of such vanadium(IV)-based magnetic cluster compounds, we recently isolated the first discrete antimony polyoxovanadates (C₆H₁₇N₃)₄[V₁₆Sb₄O₄₂] · 2H₂O, (NH₄)₄[V₁₄Sb₈O₄₂] · 2H₂O, and (trenH₃)₂[V₁₅Sb₆O₄₂] · 0.33tren · nH₂O,^{10,11} suggesting the existence of a series of substituted {V₁₈O₄₂} clusters of general composition [(amineH)_mV_{18–x}Sb_{2x}O₄₂] · nH₂O (x = 2–4).

We have now synthesized the first reduced polyoxovanadate cluster that expands the spherical {V_{18–x}Sb_{2x}O₄₂} cluster type, the first charge-neutral antimony polyoxovanadium(IV) compound [V^{IV}₁₆Sb^{III}₄O₄₂(H₂O){VO(C₆H₁₄N₂)₂]₄ · 10H₂O · C₆H₁₄N₂ (C₆H₁₄N₂ = (±)-trans-1,2-diaminocyclohexane). The central cluster fragment,

* To whom correspondence should be addressed. E-mail: wbensch@ac.uni-kiel.de.

[†] Christian-Albrechts-Universität zu Kiel.

[‡] RWTH Aachen.

- (1) Khan, M. I.; Tabussum, S.; Marshall, C. L.; Neylon, M. K. *Catal. Lett.* **2006**, *112*, 1.
- (2) Müller, A.; Reuter, H.; Dillinger, S. *Angew. Chem.* **1995**, *107*, 2505. Müller, A.; Reuter, H.; Dillinger, S. *Angew. Chem., Int. Ed. Engl.* **1995**, *34*, 2328. (c) Dong, B.; Gomez-Garcia, C. J.; Peng, J.; Benmansour, S.; Ma, J. *Polyhedron* **2006**, *26*, 1310.
- (3) Müller, A.; Sessoli, R.; Krickemeyer, E.; Bögge, H.; Meyer, J.; Gatteschi, D.; Pardi, L.; Westphal, J.; Hovemeier, K.; Rohlfing, R.; Döring, J.; Hellweg, F.; Beugholt, C.; Schmidtman, M. *Inorg. Chem.* **1997**, *36*, 5239.
- (4) (a) Chaboussant, G.; Ochsenbein, S. T.; Sieber, A.; Güdel, H.-U.; Mutka, H.; Müller, A.; Barbara, B. *Europhys. Lett.* **2004**, *66*, 423. (b) Chaboussant, G.; Basler, R.; Sieber, A.; Ochsenbein, S. T.; Desmedt, A.; Lechner, R. E.; Telling, M. T. F.; Kögerler, P.; Müller, A.; Güdel, H.-U. *Europhys. Lett.* **2002**, *59*, 291. (c) Gatteschi, D.; Pardi, L.; Barra, A. L.; Müller, A. *Mol. Eng.* **1993**, *3*, 157.

- (5) (a) Machida, M.; Miyashita, S. *Physica E* **2005**, *29*, 538. (b) Boukhvalov, D. W.; Dobrovitski, V. V.; Katsnelson, M. I.; Lichtenstein, A. I.; Harmon, B. N.; Kögerler, P. *Phys. Rev. B* **2004**, *70*, 054417.
- (6) (a) Chiorescu, I.; Wernsdorfer, W.; Müller, A.; Bögge, H.; Barbara, B. *Phys. Rev. Lett.* **2000**, *84*, 3454. (b) Kajiyoshi, K.; Kambe, T.; Mino, M.; Nojiri, H.; Kögerler, P.; Luban, M. *J. Magn. Magn. Mater.* **2007**, *310*, 1203. (c) Procissi, D.; Lascialfari, A.; Micotti, E.; Bertassi, M.; Carretta, P.; Furukawa, Y.; Kögerler, P. *Phys. Rev. B* **2006**, *73*, 184417.
- (7) (a) Müller, A.; Döring, J. *Angew. Chem.* **1988**, *100*, 1789. (b) *Angew. Chem.* **1988**, *100*, 1789; *Angew. Chem. Int. Ed. Engl.* **1988**, *27*, 1721. (c) Gatteschi, D.; Pardi, L.; Barra, A. L.; Müller, A.; Döring, J. *Nature* **1991**, *354*, 463.
- (8) Furukawa, Y.; Nishisaka, Y.; Kumagai, K.; Kögerler, P. *J. Magn. Magn. Mater.* **2007**, *310*, 1429.
- (9) (a) Tarantul, A.; Tsukerblat, B.; Müller, A. *Inorg. Chem.* **2007**, *46*, 161. (b) Tarantul, A.; Tsukerblat, B.; Müller, A. *J. Chem. Phys.* **2006**, *125*, 54714.
- (10) Kiebach, R.; Näther, C.; Bensch, W. *Solid State Sci.* **2006**, *8*, 964.
- (11) Kiebach, R.; Näther, C.; Kögerler, P.; Bensch, W. *Dalton Trans.* **2007**, 3221.

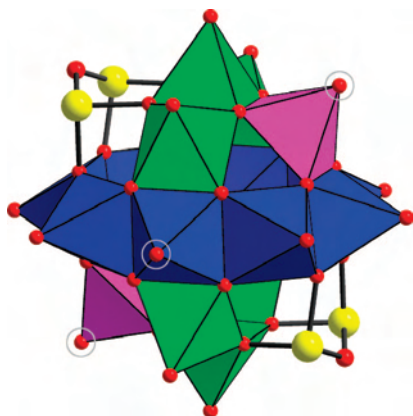


Figure 1. Polyhedral representation of the central fragment of the $[\text{V}_{16}\text{Sb}_4\text{O}_{42}(\text{H}_2\text{O})\{\text{VO}(\text{C}_6\text{H}_{14}\text{N}_2)_2\}_4]$ cluster. The VO_5 polyhedra are shown in different colors to highlight their connection. The terminal oxo groups to which additional vanadyl groups coordinate are encircled (Sb, yellow; O, red).

$[\text{V}_{16}^{\text{IV}}\text{Sb}_{16}^{\text{III}}\text{O}_{42}]$, is directly derived from the $[\text{V}_{18}\text{O}_{42}]$ archetype by replacing two VO_5 square pyramids by two Sb_2O_5 units (Figure 1).

The Sb_2O_5 units are formed by two pyramidal, corner-sharing SbO_3 groups, yielding a handlelike moiety [$\text{Sb}-\text{O}$: 1.929(3)–1.969(3) Å]. The structure of the cluster consists of two perpendicular eight-membered rings composed of edge-sharing VO_5 pyramids. Two additional VO_5 groups are located on opposite sides, and each of these VO_5 pyramids shares two edges with the two rings (Figure 1). The Sb_2O_5 units share corners with four VO_5 pyramids and edges with two VO_5 groups. As in the $\{\text{V}_{18}\text{O}_{42}\}$ structure, the 20 μ_3 -O sites [$\text{V}-\text{O}$: 1.883(3)–2.014(4) Å] span a rhombicuboctahedron. All terminal $\text{V}=\text{O}$ bond lengths are typical of vanadyl groups [$\text{V}=\text{O}$: 1.599(3)–1.673(3) Å]. The shortest $\text{V}-\text{V}$ distances are between 2.9226(8) and 3.0341(9) Å. However, the complete $\{\text{V}_{20}\text{Sb}_4\}$ structure expands the $\{\text{V}_{16}\text{Sb}_4\}$ motif by the addition of four terminal $\text{VO}(1,2\text{-diaminocyclohexane})_2$ groups featuring a slightly distorted square-pyramidal N_4VO coordination mode [$\text{V}-\text{N}$ = 2.100(4)–2.135(4) Å] with a domed VN_4 configuration, characteristic for vanadyl complexes.

The four N_4VO groups bind to four terminal O atoms of the $[\text{Sb}_{16}^{\text{III}}\text{V}_{16}^{\text{IV}}\text{O}_{42}]$ cluster (Figure 2) trans to the vanadyl $\text{V}=\text{O}$ vector and completing the final charge-neutral $[\text{V}_{16}\text{Sb}_4\text{O}_{42}(\text{H}_2\text{O})\{\text{VO}(\text{C}_6\text{H}_{14}\text{N}_2)_2\}_4]$ cluster with a diameter of approximately 17.5 Å (measured from coordinate to coordinate; Figure 2). The $\text{V}-\text{O}$ bonds to the bridging O atom [2.105(3) and 2.116(3) Å] are slightly longer than the $\text{V}-\text{O}$ bonds in the VO_5 pyramids to the O atoms of the base of the pyramids. Bond valence sum calculations indicate that all 20 V centers have an oxidation state close to 4.0.

The Sb(1) atom has two O atoms of two VN_4O groups of two neighboring clusters at 2.885 and 2.904 Å, which are shorter than the sum of the van der Waals radii.

When these weak $\text{Sb}-\text{O}$ interactions are taken into account, a three-dimensional network with different pores, which are occupied by crystal water and uncoordinated amine molecules, is formed (Figure 3). The dimensions of the channels along [100] are about 12.11 Å, along [010]

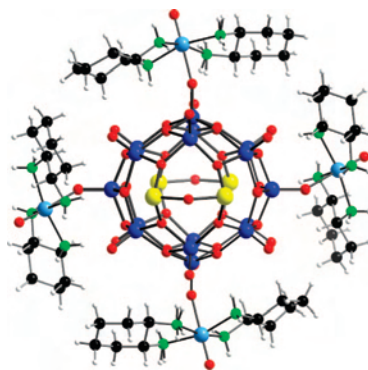


Figure 2. Structure of the $[\text{V}_{16}\text{Sb}_4\text{O}_{42}(\text{H}_2\text{O})\{\text{VO}(\text{C}_6\text{H}_{14}\text{N}_2)_2\}_4]$ cluster. The central H_2O guest molecule is not shown for clarity. V positions of the central fragment are shown in dark blue and the four terminal V centers in light blue (Sb, yellow; O, red; N, green; C, black; H, light gray).

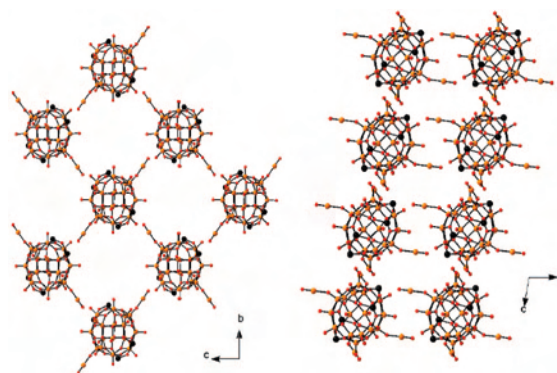


Figure 3. Arrangement of the $[\text{V}_{16}\text{Sb}_4\text{O}_{42}(\text{H}_2\text{O})\{\text{VO}(\text{C}_6\text{H}_{14}\text{N}_2)_2\}_4]$ clusters viewed along [100] (left) and along [010] (right). H_2O and organic molecules are not displayed for clarity.

11.7–12.3 Å, and along [001] 9.9–13.3 Å. The view along [100] suggests the formation of a kind of 4^4 net. The total potential solvent area calculated with the *PLATON*¹² suite is about 65.6%. Note that in the related structure of $[(\text{C}_2\text{N}_2\text{H}_{10})_2\text{-}\beta\text{-}\{\text{Sb}_8\text{V}_{14}\text{O}_{42}(\text{H}_2\text{O})\}](\text{C}_2\text{N}_2\text{H}_8)\cdot 8\text{H}_2\text{O}$ the charged clusters are joined via weak $\text{Sb}-\text{O}$ interactions ($\text{Sb}-\text{O}$: 2.794 and 2.740 Å) to form double chains.¹³ In the structure of $[(\text{Co}(\text{en})_2)_2\text{V}_{14}\text{Sb}_8\text{O}_{42}(\text{H}_2\text{O})]\cdot 8\text{H}_2\text{O}$, neighboring spherical $[\text{V}_{14}\text{Sb}_8\text{O}_{42}(\text{H}_2\text{O})]^{4-}$ clusters are bridged by the $[\text{Co}(\text{en})_2]^{2+}$ complexes, yielding charge-neutral layers.¹⁴

The magnetism is characterized by strong antiferromagnetic coupling between the $S = 1/2$ VO^{2+} groups within the central fragment, similar to the observed coupling for fully reduced $\{\text{V}_{18}\text{O}_{42}(\text{X})\}$ species.³ The low-field susceptibility is characterized by a continual decrease of χT with decreasing temperature, with values far below the high-temperature (spin-only) limit of 7.5 $\text{emu}\cdot\text{K}/\text{mol}$ for 20 uncoupled $S = 1/2$ centers ($g = 2.0$). However, the product χT approaches a shoulder at around 6 K at 1.43 $\text{emu}\cdot\text{K}/\text{mol}$ and reaches a final value of 1.4 $\text{emu}\cdot\text{K}/\text{mol}$ at 2 K, close to the spin-only value for four independent $S = 1/2$ sites (Figure 4).

(12) Spek, A. L. *PLATON*; Utrecht, The Netherlands, 2000.

(13) Zhang, L.; Zhao, X.; Xu, J.; Wang, T. J. *Chem. Soc., Dalton Trans.* **2002**, 3275.

(14) Hu, X.-X.; Xu, J.-Q.; Cui, X.-B.; Song, J. F.; Wang, T. G. *Inorg. Chem. Commun.* **2004**, 7, 264.

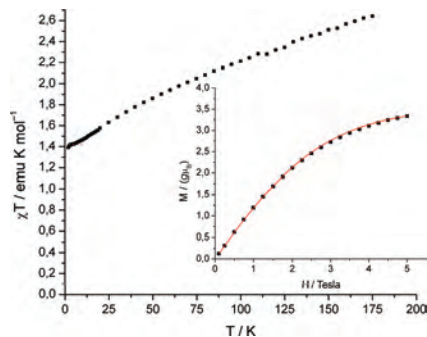


Figure 4. Temperature dependence of χT at 0.1 T for **1**. The red horizontal dots indicate the spin-only χT values for four uncorrelated spin $1/2$ centers ($g = 1.95$). Inset: Magnetization as a function of the external field at 2.0 K (experimental data, black squares; best fit to the Brillouin function, red graph).

Magnetization measurements (0–5.0 T) at 2 K confirm the existence of four uncorrelated vanadyl groups at 2 K ($g = 1.95$), and a near-perfect fit is produced by a scaled Brillouin curve $\alpha_B(S)$ with $S = 1/2$ and $\alpha = 3.89$ (Figure 4, inset). This indicates that the coupling between the terminal vanadyl groups and their neighboring V positions of the central fragment is very weak. Therefore, down to 2 K, the system can be regarded as comprising a magnetically isolated core fragment and four virtually isolated satellite spin centers.

In summary, we present the first example of a discrete reduced polyoxovanadate cage compound that has been augmented with terminal V positions, here stabilized by large chelating amine ligands. The surprising ease with which the substitution of VO_5^{6-} pyramids by $\text{Sb}_2\text{O}_5^{4-}$ groups occurs

under solvothermal conditions, even in highly stable structural archetypes such as the $\{\text{V}_{18}\text{O}_{42}\}$ cage, motivates us to probe whether other polyoxovanadate cage compounds can be substituted and/or expanded in the way presented here, too. Because the presence of polydentate organic ligands in the reaction solution is known to affect the polyoxovanadate formation mechanism,¹⁵ the nature of the employed ligand represents an additional control parameter. The charge neutrality and the addition of a lipophilic sheath of cyclohexane-based ligands render the compound soluble in various organic solvents like dimethylformamide, ethanol, methanol, and diethyldiamine, opening up new avenues for homogeneous redox catalysis. The UV–vis spectra of such solutions (Figure S2 in the Supporting Information) show strong absorption below about 400 nm.

Acknowledgment. This work was supported by the State of Schleswig-Holstein and the Fonds der Chemischen Industrie.

Supporting Information Available: Detailed experimental procedures for the synthesis, magnetic measurements, IR spectra, and UV–vis spectra of solutions of the title compound along with crystallographic data in CIF format. This material is available free of charge via the Internet at <http://pubs.acs.org>.

IC800042R

(15) Long, D.-L.; Orr, D.; Seeber, G.; Kögerler, P.; Farrugia, L.; Cronin, L. *J. Cluster Sci.* **2003**, *14*, 313.